

DOI: 10.13208/j.electrochem.130882

Artical ID:1006-3471(2014)04-0323-10

Cite this: *J. Electrochem.* **2014**, 20(4): 323-332

Http://electrochem.xmu.edu.cn

Room Temperature Ionic Liquid Templated Meso-Macroporous Material by Self-Assembled Giant Gold Nanoparticles and Its Enhancement on the Direct Electrochemistry of Cytochrome c

LI Pei¹, ZHAN Dong-ping^{1*}, SHAO Yuan-hua^{2*}

(1. *State Key Laboratory for Physical Chemistry of Solid Surfaces, College of Chemistry and Chemical Engineering, Xiamen University, Xiamen 361005, Fujian, China;*

2. *Beijing National Laboratory for Molecular Sciences, College of Chemistry and Molecular Engineering, Peking University, Beijing 100871, China)*

Abstract: Room temperature ionic liquid (RTIL) is used as a soft-template to organize a meso-macroporous material constructed by self-assembled giant gold nanoparticles which are capped by L-cysteine. First, L-cysteine capped gold nanoparticles can self-assembly to form nanowires and sub-micrometer spherical giant particles due to the static interaction and/or the condensation reaction between the carboxyl and amino groups at the outer terminal of the ligand. Second, the spherical assembled particles can form a quasi-solid gel when grinding with a hydrophobic RTIL, 1-octyl-3-methylimidazolium hexafluorophosphate. Finally, when the composite gel is coated on a glassy carbon electrode and then polarized by using cyclic voltammetry in phosphate buffer solution (PBS, pH = 7.4), a meso-macroporous structure is formed due to the leakage of the surplus of RTIL in the gel. This meso-macroporous structured material has a good conductivity and affinity to biological macromolecules. The faradaic current of cytochrome c can be enhanced significantly due to both the high outer surface area and the inner “thin-layer” effect. The experimental results indicate that this novel meso-macroporous material has potential application for electrochemical devices including biosensors and biofuel cells.

Key words: room temperature ionic liquid; self-assemble; gold nanoparticles; cytochrome c; biosensors

CLC Number: O646

Document Code: A

Porous materials have been intensively studied with regard to technical applications from chemical analysis to industrial catalysis. According to the IUPAC definition, porous materials are divided into three classes: microporous (pore size < 2 nm), mesoporous (2 ~ 50 nm) and macroporous (> 50 nm) materials^[1]. Microporous materials like zeolites have a narrow and uniform micropore size distribution due to their crystallographically defined pore system, which limits the mass transfer of reactants in-and-out of the micropores and leads to the stabilization of catalysts with larger molecular size. The advantages of

using meso-macroporous materials are the relatively large pores which can facilitate mass transport and very high surface area which allows a high concentration of active sites per mass of material. Thus, in the last decade great efforts have been made for the synthesis and application of mesoporous and macroporous materials^[2-5]. The encapsulation of enzymes and other proteins into inorganic host materials has also attracted considerable attention over the past few years. This type of research has demonstrated that biomolecules immobilized in inorganic matrixes can retain their functional characteristics to a large extent,

Received: 2013-08-23, Revised: 2013-12-11 *Corresponding author, Tel: (86- 592)2185797, E-mail: dpzhan@xmu.edu.cn, yhshao@pku.edu.cn

This work was supported by the National Natural Science Foundation of China (No. 21021002, No. 20235010, No. 20475003, No. 20420130137 and No. 20173058) and the special 985 project of the Peking University

which makes the latter attractive for application as biosensors and biocatalysts^[6].

On the other hand, nanomaterials and nanostructures have been found in many practical applications due to their unique physical and chemical properties^[7-10]. In terms of electrochemistry, metal nanoparticles can be employed to roughen the conductive sensing interface and enlarge the true reaction surface area of electrode, make a more effective contact with the redox center of large biomolecules, and enhance the direct electrochemical reactions^[11-12]. Among the reported nanomaterials, gold nanoparticles are the most facile to be obtained by a two-phase synthesis method developed by Schiffrin et al.^[13-14]. The authors also predicted that the stable gold nanoparticles could be protected by various ligands and could be functionalized at the stage of their formation. This work has stimulated researchers to assemble nanoparticles into an ensemble with controllable size, shape, and interparticle spatial properties so that the unique nanoscale properties can be effectively exploited. Apart from the immobilization of nanoparticles on different substrates using chemical assembly or LB membrane, recently some attempts have been tried to make gold nanoparticles self-assembly to reach controllably shaped and larger size^[15-18]. This provides definitely a new choice for synthesis of the mesoporous and macroporous materials which are made of self-assembled giant nanoparticles.

In general, the templates involved in the synthesis of the mesoporous and macroporous materials are the ionic surfactants, non-ionic surfactants, copolymer and nanocasting^[2]. RTILs are liquid salts of only ions at around ambient temperature, one of which is usually an ionic surfactant with a long hydrophobic chain. RTILs have some unique physical and chemical properties, such as nonvolatility, thermo-stability, good ionic conductivity and relatively wide electrochemical potential window. In recent years, significant progress has been achieved in the application of RTILs to electrochemistry^[19]. Recently, A carbon nanotube/RTILs composite gel has been found to be a good material for the direct electrochemical investi-

gation of biomolecules^[20-22]. Cytochrome c is a heme protein and consists of a single polypeptide chain of 104 amino acid residues that are covalently attached to the heme group^[23-24]. The active heme center consists of a porphyrin ring, where the four pyrrole nitrogens are coordinated to the central Fe atom forming a square planar complex. This protein is nearly spherical with a volume of $2.6 \text{ nm} \times 3.2 \text{ nm} \times 3.0 \text{ nm}$, which makes it a suitable testing biomolecule to characterize the electrochemical application of porous material, and the work was fully reviewed^[6, 25].

In this work, we report a novel meso-macroporous material composite by RTILs and self-assembled gold nanoparticles with its enhancement on the direct electrochemistry of cytochrome c. We have observed that the RTILs will leak out and a meso-macroporous structure is formed during the polarization in the phosphate buffer solution. This predicts that the RTILs could be used as a soft template to form the mesoporous and/or macroporous materials for bioelectroanalysis.

1 Experimental

1.1 Chemicals

L-cysteine, sodium borohydride (NaBH_4), hydrogen tetrachloroaurate ($\text{HAuCl}_4 \cdot 3\text{H}_2\text{O}$), sodium phosphate dibasic heptahydrate ($\text{Na}_2\text{HPO}_4 \cdot 7\text{H}_2\text{O}$), sodium phosphate monobasic monohydrate ($\text{NaH}_2\text{PO}_4 \cdot \text{H}_2\text{O}$) and sodium chloride (NaCl) were purchased from Shanghai Chemicals Co., China. Horse heart cytochrome c was provided by Aldrich. The RTILs, 1-octyl-3-methylimidazolium hexafluorophosphate ($[\text{Omin}]\text{PF}_6$), were synthesized according to the procedures described in the previous reports^[26-27] with very high purity being confirmed by ^1H NMR, and IR analyses. All chemicals were of analytical grade or better. All the aqueous solutions were prepared by twice-distilled water.

1.2 Synthesis and Characterization of Gold Nanoparticles

A homogenous phase synthesis method has been adopted since all reactants including the ligand, L-cysteine, sodium borohydride and hydrogen tetra-

chloroaurate are aqueous soluble. First, excess L-cysteine was added into the solution of hydrogen tetrachloroaurate (the molar ratio of L-cysteine to hydrogen tetrachloroaurate was 10:1) under strong stirring. A kind of light yellow gold cluster was formed and deposited. Next, the newly prepared sodium borohydride aqueous solution was added into the above mentioned solution with strong stirring. The L-cysteine capped metal gold nanoparticles were formed and the color of the solution changed into dark brown. Excess sodium borohydride was added into the solution to ensure complete reduction of the formed gold cluster. After the aqueous dispersive gold nanoparticles were centrifuged by using a high speed centrifuge (Avanti J-25, Beckman Co.), and washed thoroughly by twice-distilled water following by methanol for at least three times to remove the impurities. To characterize the gold nanoparticles, UV-Vis study was carried out with a CARY 1E spectrometer (Varian Co.). Transmission electron microscopy (TEM) was also performed by a JEOL-200CX (JEOL Co.) using the procedure reported by Chen et al.^[28-29]. The dry gold nanoparticles were collected by a rotary evaporator (Shanghai Chemicals Co.) at 30 °C.

1.3 Electrode Modification and Electrochemical Measurements

100 μL [Omin]PF₆ was mixed and ground with 180 g of L-cysteine capped gold nanoparticles using an agate mortar for about 30 minutes, and then a black gel was formed. This method is similar to the preparation of composite gel by carbon nanotubes and RTILs reported previously^[20-21]. The newly prepared meso-macroporous structure was characterized with the Quanta 200 FEG Scanning Electron Microscope (SEM, FEI Co.). A glassy carbon (GC) disk electrode (diameter of 6 mm) was polished with alumina powder, and then was sequentially washed in twice distilled water and ethanol. The GC electrode was characterized by 0.1 mmol $\cdot\text{L}^{-1}$ potassium ferricyanide with a peak potential difference of 60 mV under the sweep rate of 20 ms. The gold nanoparticles/RTILs composite gel was placed on a smooth glass slide.

The GC electrode was rubbed over the gel, and the gel was mechanically attached to the surface. The gel on the electrode surface was further smoothed with a spatula to form a thin and uniform gel film on the GC electrode surface (ca. 50 ~ 100 $\mu\text{mol} \cdot \text{L}^{-1}$ thick estimated by the optical microscopy, BX-51, Olympus). Then, the gel modified GC electrode was ready for electrochemical experiments. A platinum wire was employed as the counter electrode and a saturated calomel electrode was adopted as the reference electrode. The solutions were purged with highly purified nitrogen for at least 20 minutes prior to the experiments. Nitrogen atmosphere was maintained over the solutions during the experiments. All the electrochemical experiments were carried out by using a CHI 660A electrochemical workstation (CH Instruments Co.) at room temperature ((20 \pm 2) °C).

2 Results and Discussion

2.1 Self-Assembly of the L-Cysteine Capped Gold Nanoparticles

To obtain the size-controllable and uniform gold nanoparticles, a ligand is usually adopted to stabilize the nanoparticles through either the covalent or static interactions. For further modification or assembly of the gold nanoparticles, it is also essential to use bi-functional thioether-containing molecules which have another functional group on the other terminal. L-cysteine is chosen here as the protection ligand because it contains a thiol group and can be chemically adsorbed on the surface of gold nanoparticles without congregation. Under our experimental conditions, the uniform sized gold nanoparticles can be obtained. On the other hand, it also has two other functional groups: carboxyl and amino groups. The gold nanoparticles are aqueous soluble due to its tiny size and the strong hydrophilicity of the both outward groups. It takes several weeks to observe the deposition in the aqueous solution of the gold nanoparticles when stored in a freezer at 4 °C. Generally, the two groups which are adsorbed on different particles can combine with each other through the electrostatic interaction and further chemical reaction. As a result, the L-cysteine capped nanoparticles are self-assem

bled and appeared as grainy, linear and sphere forms as depicted in Fig. 1. The UV-Vis spectrum (Fig. 1A) shows an adsorption peak at 520 nm for the newly synthesized nanoparticles after strong sonicated, which is the characteristic peak of the single gold nanoparticle^[18]. Fig. 1B shows the TEM image of the newly prepared nanoparticles which appear as single granules and also some congregating features. The average size of the gold nanoparticles is less than 10 nm. If the aqueous dispersible gold nanoparticles are reserved for 12 hours at room temperature, a linear cross-linking feature can be observed in the TEM image (see Fig. 1C). Even larger sphere assemblies with an average diameter of 100 nm can be observed as a deposition after reserved for three days at room temperature (Fig. 1D). When the self-assembled gold nanoparticles are strongly sonicated for several hours, the deposition in aqueous solution disappears and the cross-linking behavior similarly to the case shown in Fig. 1C can be seen again. We have also changed the depositing time and the molar ratio between L-cysteine and hydrogen tetrachloroaurate from 10:1 to 100:1, the sizes of the assembled larger particles are of (100 ± 20) nm and no obvious change is observed. The results show that the size is mainly dependent upon the surface charges of the gold nanoparticles and their interactions. The value of 100 nm might be the most stable size when the molar ratio between L-cysteine and hydrogen tetrachloroaurate is more than 10:1. It can also conclude that the spherical structure is much stable than the cross-linking one due to the distribution of the surface charges. In other words, the surface Gibbs energy might be minimized in the case of spherical assembly. These phenomena are in accordance with the recently work by Zhong et al. They reported that the nanoparticles could form the cross-linking assembly through the hydrogen bonding between the carboxyl acid groups or form the sphere structure through multidentate thioethers^[15-17]. The same system as ours was also reported and gave a preliminary explanation for the giant spherical assembly. They considered that the terminal amino group would adsorb on the neighbor gold nanoparti-

cle if an appropriate pH value is controlled, which is the same mechanism as the case of assembly through the dithiol ligands^[18]. However, the cysteine molecule is so small that there are only four atoms in the carbon chain. It is suspect that the adsorptive energy is enough to balance the repulsive force between the two negatively recharged gold nanoparticles based on the previous report that the length of the carbon chain is no less than 6 can form a stable gold nanoparticle^[14]. In this work, the pH of the solution during the whole experiment was not controlled, but the linear cross-link and spherical self-assembly of L-cysteine capped gold nanoparticles can still be observed. Here we propose that the driving force of the self-assembly of L-cysteine capped gold nanoparticles is due to the chemical interaction between the outer terminal groups as depicted in Fig. 2. It is well known that the thiol has stronger adsorptive capability than amino groups with Au. Although the L-cysteine can dimerize to form systin, only the interactions between the carboxylic acid groups and/or amino groups are focused in the case of self-assembly: (i) the hydrogen bond between the carboxylic acid groups on the neighbor gold nanoparticles. Under certain circumstance the two molecules may lose a H_2O to produce ester. (ii) the condensation reaction between the carboxylic acid and the amino group to form the oligomer of peptides. And the product has a hydrogen bond within the molecule which makes it very stable. (iii) the condensation reaction between the carboxylic acid and the amino group to form a hexacyclic structure. The simulation by ChemSketch shows that it is stable and has proved by the synthetic chemistry of cyclic peptides^[30-32]. When an aqueous solution of L-cysteine was sealed and placed in room environment for a few days, a white insoluble mixed product can be obtained. The organic spectrum results show that the reaction II gives the main products (see the supporting materials). The L-cysteine adsorbed on the nanoparticles acts as a thread to link the pears into a necklace. And it finally becomes a sub-mirometer ball due to the minimization of the surface energy. The results are in accordance with the routine from linear to

spherical assembly as reported by Zhong et al.^[18] which is also reviewed by Nayak and Lyon^[33].

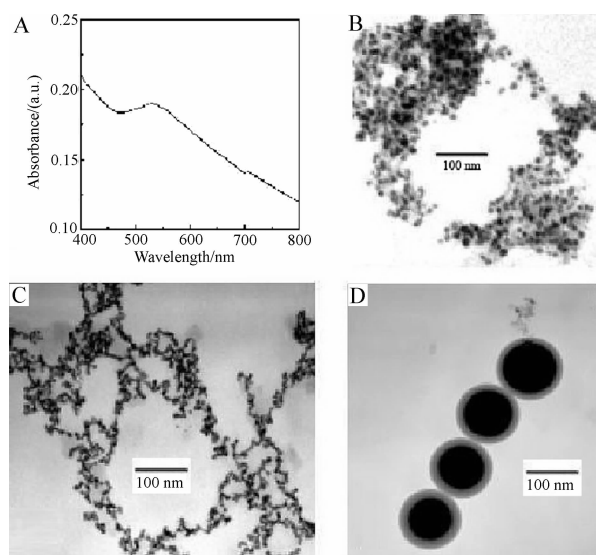


Fig. 1 Characterization of the L-cysteine capped nanoparticles: the UV-vis spectrum of the newly prepared gold nanoparticles (A); the respective TEM images of the newly prepared (B), 12 hours deposited (C) and three days deposited gold nanoparticles (D) at room temperature

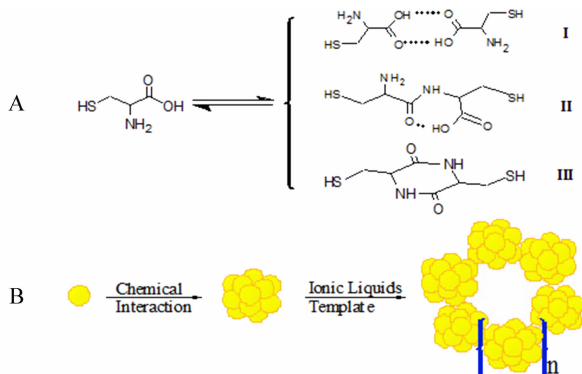


Fig. 2 The interaction between L-cysteine on the neighbor gold nanoparticles (A) and the schematic routine of the formation of the giant self-assembled gold nanoparticles and the meso-macroporous structure templated by RTILs (B)

2.2 Formation of the Meso-Macroporous Structure Templated by [Omin]PF₆

When the dry capped gold nanoparticles were grounded with [Omin]PF₆, a black quasi-solid gel was

formed. The fully-ground gel was coated on a glassy carbon electrode. Then, the newly prepared electrode was immersed in the phosphate buffer solution (pH = 7.4) and polarized in a certain potential region by cyclic voltammetry repeatedly until the double-layer charging/discharging voltammograms became stable and no longer changed with time. In contrast to a conventional electrode/solution interface, this gel modified electrode is composed of a high charge-density quasi-solid soft material, which contains both hydrophilic and hydrophobic domains. When the composite gel electrode contacts with the aqueous electrolyte, the electrode/solution interface will be reorganized inevitably during the continuous polarization. At the beginning of the scan, the double-layer charging/discharging voltammograms were distorted which show an obviously big *IR* drop and a relatively small double-layer capacity. After scan for more than 10 minutes, the voltammogram was not changed any more and showed a less *IR* drop but a bigger capacity. It means that the high dielectric RTILs leaked out during the continuous scan and the gel was transferred into a meso-macroporous structure. As a result, the electric resistance of the modified layer was reduced. At the same time the double layer capacity of the electrode/solution interface was enlarged due to the enlarged specific surface. Experimentally, the double layer will be charged/discharged continuously until a steady state of the electrode/solution interface is achieved, which has essentially the smallest *IR* drop voltammetrically.

The meso-macroporous structure of giant self-assembly gold nanoparticles templated by RTILs could be proved by the SEM micrograph as shown in Fig. 3. The bright regions represent the nonleaky ionic liquids and the tiny granules are the self-assembled gold nanoparticles. The ionic liquids provide a pure ionic strength atmosphere to disperse the assembled gold nanoparticles. Accordingly, the surface charge of the giant particles is optimized and the surface energy of the particles is minimized. It can be observed that the giant particles are surrounded by a tiny thin layer of the RTILs and the stable size of which is e-

qual to (100 ± 20) nm. The RTILs leak away from the gel during the polarization. As a result, the giant self-assembled gold nanoparticles have formed a three-dimensional porous structure as shown in the Fig. 3. The diameters of the pores vary from 30 nm to 600 nm, which is the hybrid of mesoporous and macroporous, and defined as meso-macroporous structure. A more homogeneous porous structure would be expected if the technique of gel fabrication had been optimized, which includes the optimized parameters such as the ratio of the RTILs to gold particles, the time of grinding, and so forth.

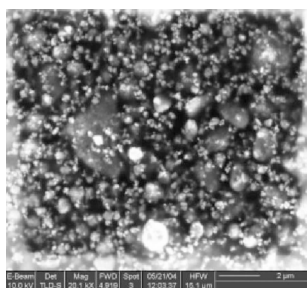


Fig. 3 The SEM image of the gold nanoparticles/ionic liquid composite gel (scale bar is $2 \mu\text{mol} \cdot \text{L}^{-1}$, and the accelerating voltage is 10.0 kV)

Similar to our previous work on the meso-macroporous structure composite by the multiwall carbon nanotubes (MWNTs) templated by RTILs^[20-21], the double layer charging currents of meso-macroporous electrode of giant gold nanoparticles templated by RTILs are much higher than those of the bare GC electrode. This may be contributed to the following factors: (i) the gold nanoparticles are capped by a layer organic molecules of L-cysteine, which is similar to the conventional thin film capacitors; (ii) the non-electron conductivity and high dielectric coefficient of the ionic liquid will significantly increase the capacitance; (iii) the high specific surface of the meso-macroporous material will definitely enhance the double layer capacity. However, the following experimental results prove that the large double layer capacity will not disturb the measurement of faradaic current of cytochrome c due to the enhancement effect.

2.3 Enhancement on Direct Electrochemical Reaction of Cytochrome c

A conventional three-electrode system is employed to investigate the electrochemical behavior of cytochrome c on the composite modified electrode. When the pre-treated electrode is moved into the solution with cytochrome c, the typical cyclic voltammograms are shown in Fig. 4. It is clearly that the anodic current is approximately equal to the cathodic one. The peak currents are proportional to the square roots of the sweep rates in a certain range. The difference of the peak potentials is slightly increased with the sweep rate. These results show phenomenally that the redox reaction of cytochrome c on this composite modified electrode seems to be a quasi-reversible process. When the sweep rate is faster than $200 \text{ mV} \cdot \text{s}^{-1}$, the voltammogram will be distorted due to the high value of double layer capacitance and the uncompensated IR drop. From Fig. 4 we notice that the influence of the double-layer capacitance is not so large. As demonstrated previously, the composite electrode has a meso-macroporous structure. When a redox couples are added and penetrate into the inner porous structure, the dielectric coefficient of solution will be changed, which results in a change of double layer capacity. On the other hand, the faradaic current will be enhanced due to large specific surface of the porous structure. As a matter of fact, the ratio in charging current of double layer to faradaic current apparently decreases.

If the surface of the electrode is supposed to be uniformed, the relationship among the peak currents, the concentrations and the square roots of the sweep rate should follow the Randles-Sevcik equation, which is suitable for the case of semi-infinite diffusion controlled system^[34].

$$i_p = 0.4463 \times 10^{-3} (nF)^{3/2} A (RT)^{-1/2} D^{1/2} C v^{1/2} \quad (1)$$

where i_p is the anodic peak current, n is the transferred electron numbers of the reaction, F is the Faraday constant, A is the area of the electrode, R is the gas constant, T is the absolute temperature, D is the diffusion coefficient of cytochrome c, C is the concentration of cytochrome c, v is the sweep rate.

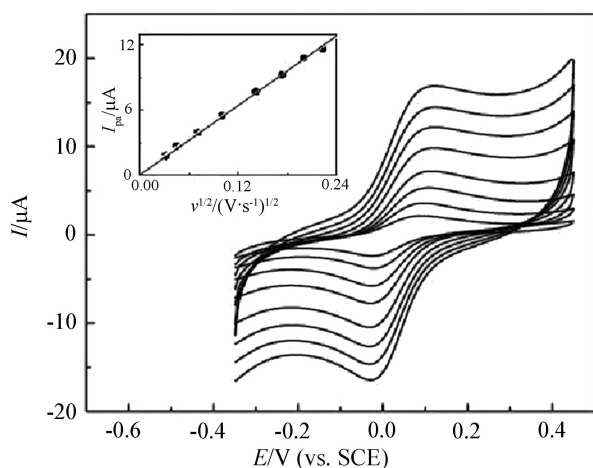


Fig. 4 The cyclic voltammograms of $0.2 \text{ mmol} \cdot \text{L}^{-1}$ cytochrome c in $25 \text{ mmol} \cdot \text{L}^{-1}$ phosphate buffer solution ($\text{pH} = 7.4$) with the sweep rates of 1, 2, 5, 10, 20, 30, 40, 50 $\text{mV} \cdot \text{s}^{-1}$ (the insert is the linear relationship between the anodic peak current and the square root of the sweep rate)

From the linear relationship between the peak current and the square roots of the sweep rate (the insert of Fig. 4), the diffusion coefficient of cytochrome c in the aqueous solution can be calculated to be $(9.1 \pm 0.3) \times 10^{-6} \text{ cm}^2 \cdot \text{s}^{-1}$. This value is more than ten times larger in magnitude than the one reported previously^[35-36]. Generally, the diffusion coefficient is a thermodynamic parameter, which should keep constant in the chosen solution. The result can only be explained by the meso-macroporous structure of the composite electrode. First, the true active area of the composite electrode should be much larger than its geometrical area. During the pre-polarization, the specific surface of the composite electrode is enlarged significantly because of the leakage of the ionic liquids (as shown in Fig. 3). Since the calculation is based on the geometric surface area of the electrode regardless the porous ratio and thickness of the modified layer, definitely the resulted diffusion coefficient is much larger than the reported value. Second, the reported diffusion coefficient is obtained from one dimensional diffusion process at a conventional electrode. On this composite electrodes, cytochrome c can diffuse onto the reaction centers of the sub-micrometer sized particles, which is a 3-dimensional nanoscale process

and can significantly enhance the unit mass transport rate. This phenomenon has been theoretically analyzed for the enhancement of mass transport at ultra microelectrodes^[37]. Furthermore, since the diffusion layers of the neighbor particles are overlapped each other, it could be considered that the process in the porous structure just as electrolysis in a thin layer. The faradaic current of inner thin layer is in proportion to the scan rate and has a narrower peak potential difference. This is why the current peaks are rather nice and the difference in the peak potentials is even less than 60 mV at a scan rate slower than $1 \text{ mV} \cdot \text{s}^{-1}$.

This composite modified electrode is sensitive to cytochrome c and the amount as low as $1 \text{ } \mu\text{mol} \cdot \text{L}^{-1}$ can be determined when the differential pulse voltammetry is employed (see Fig. 5). The peak current shows good linearity to the concentration of cytochrome c from 1 to $200 \text{ } \mu\text{mol} \cdot \text{L}^{-1}$. Another advantage of this composite gel modified electrode is the good stability. Fig. 6 shows the voltammograms of the initial cycle and the cycles scanned after three hours, in which no significant changes are observed. This is because $[\text{Omim}]\text{PF}_6$ is very hydrophobic and viscous, which covers on the surface of giant gold nanoparticles and binds them each other to form a stable meso-macroporous structure. In our previous work on MWNTs/RTILs composite electrode, hemoglobin absorbs on the porous structure and a pair of redox current peaks can be observed even after the electrode is rinsed by PBS and then polarized in PBS. In the present work no such phenomenon is observed. When the electrode is rinsed by PBS and polarized in PBS, no faradaic current can be observed. It can be concluded that the molecules of cytochrome c can diffusion to-and-from the meso-macroporous structure and the enhanced faradaic current is due to the thin layer effect rather than absorption. This is different from those reported by McKenzie et al.^[38-39] who have demonstrated ambiguously that the enhancement was attributed to the absorption of cytochrome c as an “ideal” thin layer. Since no special absorption occurs in our experiment, the electrode could be recovered

and used repeatedly. The results show that the unique gel modified electrode is suitable for the development of electrochemical devices^[40-42].

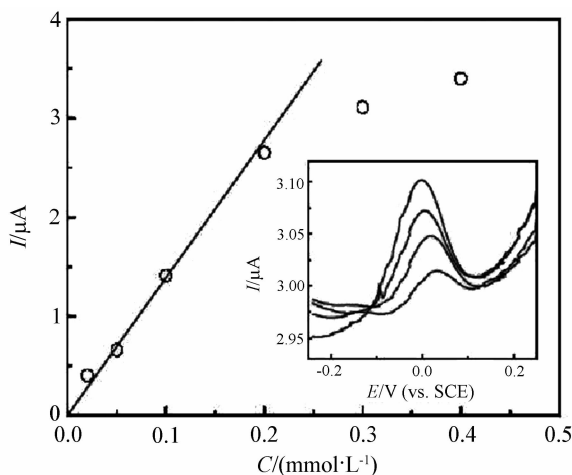


Fig. 5 The relationship between the faradaic current measured by differential pulse voltammetry and the concentration of cytochrome c (the insert shows the differential pulse voltammograms at the low concentrations of cytochrome c: 2, 4, 6, 8 $\mu\text{mol}\cdot\text{L}^{-1}$)

Sweep rate: $20\text{ mV}\cdot\text{s}^{-1}$; Pulse amplitude: 50 mV ; Sample width: 20 ms ; Pulse width: 50 ms ; Pulse period: 200 ms

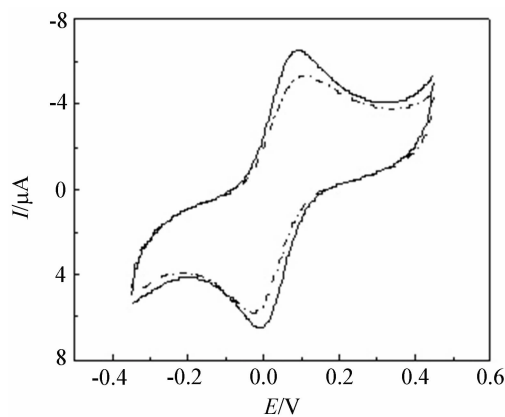


Fig. 6 The cyclic voltammograms of $0.2\text{ mmol}\cdot\text{L}^{-1}$ cytochrome c in $25\text{ mmol}\cdot\text{L}^{-1}$ phosphate buffer solution ($\text{pH} = 7.0$) (the solid line is the initial scanning cycle and the dot line is the one after three hours) Sweep rate: $5\text{ mV}\cdot\text{s}^{-1}$

3 Conclusions

This paper reports that (i) The L-cysteine capped

gold nanoparticles can self-assembled from linear to spherical sub-micrometer beads, the driving force is the interaction between the outward carboxyl acid and/or amino groups; (ii) The room temperature ionic liquids can disperse and stabilize the self-assembled spherical giant gold particles to form a soft quasi-solid gel through the mechanic grinding; (iii) When the gel modified electrode is polarized in phosphate buffer solution, the excess room temperature ionic liquids will leak out from the gel to form a meso-macroporous structure; (iv) This meso-macroporous material has a good affinity and stability for biomolecules. The direct electrochemical reaction of cytochrome c can be significantly enhanced due to the nano-scale roughness of the outer surface and the inner thin layer effect. The results show that this type of material is a good candidate for fabrication of electrochemical devices from sensors to biofuel cells.

References:

- [1] Sing K S W, Everett D H, Haul R A W, et al. Reporting physisorption data for gas/solid systems with special reference to the determination of surface area and porosity[J]. Pure and Applied Chemistry, 1985, 57(4): 603-619.
- [2] Yuan Z, Su B. Insights into hierarchically meso-macroporous structured materials[J]. Journal of Materials chemistry, 2006, 16(77): 663-677.
- [3] Taguchi A, Schuth F. Ordered mesoporous materials in catalysis[J]. Microporous and Mesoporous Materials, 2005, 77(1): 1-45.
- [4] Schuth F. Engineered porous catalytic materials[J]. Annual Reviews Materials Research Innovations, 2005, 35: 209-238.
- [5] Van de Water, Leon G A, Maschmeyer T. Mesoporous membranes-a brief overview of recent developments [J]. Topics in Catalysis, 2004, 29(2): 67-77.
- [6] Hartmann M. Ordered Mesoporous Materials for bioadsorption and biocatalysis[J]. Chemistry of Materials, 2005, 17(18): 4577-4593.
- [7] Brust M, Kiely C J. Some recent advances in nanostructure preparation from gold and silver particles: A short topical review[J]. Colloids and Surfaces A: Physicochemical and Engineering Aspects 2002, 202(2/3): 175-186.
- [8] Shipway A N, Katz E, Willner I. Nanoparticle arrays on surfaces for electronic, optical, and sensor applications[J]. Chemical Physics and Physical Chemistry, 2000, 1 (1):

- 18-52.
- [9] Daniel M C, Astruc D. Gold nanoparticles: Assembly, supramolecular chemistry, quantum-size-related properties, and applications toward biology toward biology, catalysis, and nanotechnology[J]. Chemical Reviews, 2004, 104(1): 293-346.
- [10] Buzzeo M C, Evans R G, Compton R G. Non-haloaluminate room-temperature ionic liquids in electrochemistry-a review[J]. Chemical Physics and Physical Chemistry, 2004, 5(8): 1106-1120.
- [11] Santos D H, Garcia M B, Garcia A C. Metal-nanoparticles based electroanalysis[J]. Electroanalysis, 2002, 14(18): 1225-1235.
- [12] Katz E, Willner I, Wang J. Electroanalytical and bioelectroanalytical systems based on metal and semiconductor nanoparticles[J]. Electroanalysis, 2004, 16(1/2): 19-44.
- [13] Brust M, Fink J, Bethell D, et al. Synthesis and reactions of functionalized gold nanoparticles[J]. Journal of the Chemical Society-Chemical Communications, 1995, 16: 1655-1656.
- [14] Templeton A C, Wuelfing W P, Murray R W. Monolayer-protected cluster molecules[J]. Accounts of Chemical Research, 2000, 33(1): 27-36.
- [15] Zheng W, Maye M M, Leibowitz F L, et al. Imparting biomimetic ion-gating recognition properties to electrodes with a hydrogen-bonding structured core-shell nanoparticle network[J]. Analytical Chemistry, 2000, 72(10): 2190-2199.
- [16] Maye M M, Chun S C, Han L, et al. Novel spherical assembly of gold nanoparticles mediated by a tetradentate thioether[J]. Journal of the American Chemical Society, 2002, 124(18): 4958-4959.
- [17] Maye M M, Lim I S, Luo J, et al. Mediator-template assembly of nanoparticles[J]. Journal of the American Chemical Society, 2005, 127(5): 1519-1529.
- [18] Zhong Z, Subramanian A S, Highfield J, et al. From discrete particles to spherical aggregates: A simple approach to the self-assembly of Au colloids[J]. Chemistry-A European Journal, 2005, 11(5): 1473-1478.
- [19] Ohno H. Electrochemical aspects of ionic liquids[M]. John Wiley & Sons, Inc., Hoboken, New Jersey, 2005.
- [20] Zhao Q, Zhan D, Ma H, et al. Direct proteins electrochemistry based on ionic liquid mediated carbon nanotube modified glassy carbon electrode[J]. Frontiers in Bioscience, 2005, 10(1): 326-334.
- [21] Zhao Y, Gao Y, Zhan D, et al. Selective detection of dopamine in the presence of ascorbic acid and uric acid by a carbon nanotubes-ionic liquid gel modified electrode[J]. Talanta, 2005, 66(1): 51-57.
- [22] Zhao F, Wu X, Wang M, et al. Electrochemical and bioelectrochemistry properties of room-temperature ionic liquids and carbon composite materials[J]. Analytical Chemistry, 2004, 76(17): 4960-4967.
- [23] Harbury H A, Loach P A. Oxidation-linked proton functions in hem octa- and undecapeptides from mammalian cytochrome c[J]. Journal of Biological Chemistry, 1960, 235: 3640-3647.
- [24] Senn H, Wüthrich K. Amino acid sequence, heme-iron coordination geometry and functional properties of mitochondrial and bacterial c-type cytochromes[J]. Quarterly Reviews of Biophysics, 1985, 18(2): 111-118.
- [25] Alain Walcarius. Impact of mesoporous silica-based materials on electrochemistry and feedback from electrochemical science to the characterization of these ordered materials[J]. Comptes Rendus Chimie, 2005, 8(3/4): 693-712.
- [26] Huddleston J G, Willauer H D, Swatowski R P, et al. Room temperature ionic liquids as novel media for 'clean' liquid-liquid extraction[J]. Chemical Communications, 1998, 16: 1765-1766.
- [27] Ma H, Wan X, Chen X, Zhou Q. Reverse atom transfer radical polymerization of methyl methacrylate in room-temperature ionic liquids[J]. Journal of Polymer Science, Part A: Polymer Chemistry, 2002, 41(1): 143-147.
- [28] Chen S W. 4-Hydroxythiophenol-protected gold nanoclusters in aqueous media[J]. Langmuir, 1999, 15(22): 7551-7557.
- [29] Chen S W. Nanoparticle assemblies. "Rectified" quantized charging in aqueous media[J]. Journal of the American Chemical Society, 2000, 122(30): 7420-7421.
- [30] Amarin M, Castedo L, Granja J R. New cyclic peptide assemblies with hydrophobic cavities: The structural and thermodynamic basis of a new class of peptide nanotubes[J]. Journal of the American Chemical Society, 2003, 125(30): 2844-2845.
- [31] Rosenthal-Aizman K, Svensson C, Uden A. Self-assembling peptide nanotubes from enantiomeric Pairs of cyclic peptides with alternating D and L amino acid residues[J]. Journal of the American Chemical Society, 2004, 126(11): 3372-3373.
- [32] Nakayama K, Kawato H C, Inagaki H, et al. Novel peptidomimetics of the antifungal cyclic peptide Rhodopeptin: Design of mimetics utilizing scaffolding methodology[J]. Organic Letters, 2001, 3(22): 3447-3450.
- [33] Nayak S, Lyon L A. Soft nanotechnology with soft nanoparticles[J]. Angewandte Chemie International Edition, 2005, 44(47): 7686-7708.

- [34] Bard A J, Faulkner L R. Electrochemical methods: Fundamentals and applications (2nd edition)[M]. John Wiley & Sons, 2001: 231.
- [35] Fedurco M C. Redox reactions of heme-containing metalloproteins: Dynamic effects of self-assembled monolayers on thermodynamics and kinetics of cytochrome c electron-transfer reactions [J]. Coordination Chemistry Reviews, 2000, 209: 263-286.
- [36] Sevilla J M, Pineda T, Roman A J, et al. The direct electrochemistry of cytochrome c at a hanging mercury drop electrode modified with 6-mercaptopurine[J]. Electroanalytical Chemistry, 1998, 451(1/2): 89-93.
- [37] Fleischmann M. Ultramicroelectrodes and fabrications [M]//Fleischmann M, Pons S, Robinson D R, et al (Eds). Ultramicroelectrodes. London: Systems Press, 1987.
- [38] McKenzie K J, Marken F, Opallo M. TiO₂ phytate films as hosts and conduits for cytochrome c electrochemistry [J]. Bioelectrochemistry, 2005, 66(1/2): 41-47.
- [39] McKenzie K J, Marken F. Accumulation and reactivity of the redox protein cytochrome c in mesoporous films of TiO₂ phytate[J]. Langmuir, 2003, 19(10): 4327-4311.
- [40] Ikeda T, Kano K J. An electrochemical approach to the studies of biological redox reactions and their applications to biosensors, bioreactors, and biofuel cells [J]. Journal of Bioscience and Bioengineering, 2001, 92(1): 9-18.
- [41] Wilner I, Willner B. Biomaterials integrated with electronic elements: en route to bioelectronics[J]. Trends in Biotechnology, 2001, 19(6): 222-230
- [42] Ikeda T, Kano K. Bioelectrocatalysis-based application of quinoproteins and quinoprotein-containing bacterial cells in biosensors and biofuel cells [J]. Biochimica Et Biophysica Acta-Proteins and Proteomics, 2003, 1647(1/2): 121-126.

离子液体/金纳米粒子自组装介孔材料及其增强的细胞色素 c 直接电化学

李 培¹, 詹东平^{1*}, 邵元华^{2*}

(1. 厦门大学 化学化工学院, 固体表面物理化学国家重点实验室, 福建 厦门 361005;

2. 北京大学 化学与分子工程学院, 分子科学国家实验室, 北京 100871)

摘要: 室温离子液体作为一种软模板用来组装介孔材料, 这种材料是由表面覆盖有半胱氨酸的自组装巨型金纳米粒子构成的。首先, 由于静电作用或者配体末端的羧基和氨基基团之间的缩合反应, 覆盖有半胱氨酸的金纳米粒子能够自组装形成纳米线和亚微米球形粒子。其次, 球形自组装粒子在和疏水性室温离子液体 1-辛基-3-甲基咪唑鎓六氟磷酸盐相互研磨时能形成一种准固态凝胶。最后, 将复合凝胶涂在玻碳电极上, 然后在 PH=7.4 的磷酸缓冲溶液中用循环伏安法进行极化, 由于富余的室温离子液体分散在溶液中, 形成了一种介孔组装结构。该材料具有良好的导电性和生物大分子亲和性。由于比表面积大和介孔内部的“薄层”效应, 细胞色素 c 的氧化还原反应显著增强。实验结果表明, 这种介孔材料在生物传感器和生物燃料电池等电化学器件方面具有潜在的应用前景。

关键词: 室温离子液体; 自组装; 金纳米粒子; 细胞色素 c; 生物传感器